Inorg. Chem. **2007**, *46*, 1627–1633

First-Row Transition-Metal Complexes Based on a Carboxylate Polychlorotriphenylmethyl Radical: Trends in Metal–Radical Exchange Interactions

Daniel Maspoch,[†] Neus Domingo,[‡] Daniel Ruiz-Molina,[†] Klaus Wurst,[§] Joan Manel Hernández,[‡] Francesc Lloret,[£] Javier Tejada,[‡] Concepció Rovira,[†] and Jaume Veciana*,[†]

Institut de Ciència de Materials de Barcelona, CSIC, Campus Universitari de Bellaterra, 08193 Cerdanyola, Spain, Facultat de Física, Universitat de Barcelona, Diagonal 647, 08028 Barcelona, Spain, Institut für Allgemeine, Anorganische und Theoretische Chemie, Universität Innsbruck, Innrain 52a, A-6020 Innsbruck, Austria, and Departament de Química Inorgànica/Instituto de Ciencia Molecular, Facultat de Química de la Universitat de València, Dr. Moliner 50, E-46100 Burjassot, València, Spain

Received September 23, 2006

We report the synthesis, crystal structures, and magnetic properties of a series of mononuclear, metal–radical complexes with first-row transition-metal ions using a new class of radical-based ligands, the polychlorinated triphenylmethyl (PTM) radicals. Crystal structures of three new PTM-based complexes of general formula $M(PTMMC)_2(py)_{4-x}(H_2O)_x$ [PTMMC = PTM radical functionalized at the *para* position with one carboxylic group; M = Zn(II), $x = 2$ (**1**); M = Ni(II), $x = 1$ (**2**); M = Co(II), $x = 1$ (**3**)] show similar molecular structures in which mononuclear complexes are formed by an octahedral metal ion coordinated by two monodentated PTMMC units. From a magnetic point of view, these similar configurations describe a quasilinear, trimeric magnetic model (PTMMC–M(II)–PTMMC), in which the metal [Ni(II) or Co(II)]–radical magnetic-exchange coupling constants have been determined for the first time. In all of these complexes, the temperature dependence of the magnetic susceptibility reveals moderate antiferromagnetic-exchange coupling constants between the PTMMC radicals and Ni(II) ($2J/k_B = -47.1$ K) and Co(II) ions ($2J/k_B = -15.2$ K) based on the exchange Hamiltonian $H = -2JS_M(S_{rad1} + S_{rad2})$.

Introduction

The so-called "metal−radical approach" has become an imaginative and successful strategy to obtain a wide range of metal−organic magnetic molecular materials.[1−3] Such an approach, which is based on the combination of magnetically active transition-metal ions and persistent organic radicals as ligands, enhances the strength of magnetic interactions and, therefore, the magnetic dimensionality of the molecular material in comparison with that of systems made up from paramagnetic metal ions and diamagnetic coordinating ligands. For this reason, it is reasonable to imagine that the design and synthesis of new stable organic radicals capable of acting as paramagnetic ligands is one of the most important challenges within this strategy. So far, nitroxide-based radicals[4] in the form of nitronyl or imino nitroxides,[5−10] polynitroxides,[11,12] or functionalized with carboxylic-based[13] and/or N-based ligating groups[8,14] have played a prominent

* To whom correspondence should be addressed. E-mail: vecianaj@icmab.es. Telephone: +34 93 5801853. Fax: +34 93 5805729.
[†] Institut de Ciència de Materials de Barcelona.
[‡] Universitat de Barcelona.
[§] Universität Innsbruck.
[£] Universitat de València.

(1) Caneschi, A.; Gatteschi, D.; Sessoli, R.; Rey, P. *Acc. Chem. Res.* **1989**, *22*, 392.
(2) Caneschi, A.; Gatteschi, D.; Rey, P. *Prog. Inorg. Chem.* **1991**, *39*, 331.
(3) Iwamura, H.; Inoue, K.; Hayamizu, T. *Pure Appl. Chem.* **1996**, *68*, 243.
(4) Iwamura, H.; Inoue, K. In *Magnetism: Molecules to Materials II*; Miller, J. S., Drillon, M., Eds.; Wiley-VCH: New York, 2001.
(5) Laugier, J.; Rey, P.; Benelli, C.; Gatteschi, D.; Zanchini, C. *J. Am. Chem. Soc.* **1986**, *108*, 6931.
(6) Oshio, H.; Ito, T. *Coord. Chem. Rev.* **2000**, *198*, 329.
(7) Rancurel, C.; Sutter, J.-P.; Le Hoerff, T.; Ouahab, L.; Kahn, O. *New J. Chem.* **1999**, 1333.
(8) Marvilliers, A.; Pei, Y.; Cano, J.; Vostrikova, K. E.; Paulsen, C.; Rivière, E.; Audière, J.-P.; Mallah, T. *Chem. Commun.* **1999**, 1951.
(9) Field, L. M.; Lahti, P. M.; Palacio, F. *Chem. Commun.* **2002**, 636.
(10) Stroh, G.; Turek, P.; Rabu, P.; Ziessel, R. *Inorg. Chem.* **2001**, *40*, 5334.
(11) Inoue, K.; Iwamura, H. *J. Chem. Soc., Chem. Commun.* **1994**, 2273.
(12) Inoue, K.; Iwamura, H. *Adv. Mater.* **1996**, *8*, 73.

10.1021/ic061815x CCC: $37.00
Published on Web 02/08/2007

role in the development of this approach. This broad range of coordination functionalities has allowed the construction of multiple magnetic molecular materials, evolving from 0-D to 3-D systems with a great diversity of magnetic properties, such as ferro-,[15] ferri-,[16,17] meta-,[18] and antiferromagnetic,[19] 1-D single-chain magnetic behavior,[20] and spin-frustation[21] and spin-glass behavior,[22] among others. Other open-shell radical ligands that have also been successfully used within the metal−radical approach are (a) derivatives of the verdazyl radical family, which turned out to be very attractive because of their abundance of donor atoms and efficiency in transmitting magnetic interactions,[23,24] (b) *o*-quinone ligands that can be found in different accessible oxidation states, including the radical semiquinones (SQ-) oxidation state,[25−27] (c) tetracyanoethylene (TCNE) and tetracyanoquinone (TCNQ) radical anions,[28] and (d) diphenylcarbenes substituted with chemical functions able to coordinate with metal ions.[29,30] However, even though the description of these families has become an excellent contribution to the metal−organic approach, it is obvious that the variety of radical-based ligands used, up to now, is fairly limited.

Our contribution to this field focuses mainly on the use of a new type of free, open-shell ligands based on polychlorinated triphenylmethyl radicals (PTM) properly functionalized with carboxylic groups. The interest for these radicals is twofold. First, PTM radicals exhibit an astonishing life expectancy and thermal and chemical stability,[31] and second, they can be easily functionalized with one or more coordinating groups, opening new routes for the design of multidimensional magnetic molecular materials.[32−35] According to these expectations, a new tricarboxylic PTM radical has already been used to obtain a series of one- and two-dimensional metal−organic materials (MOROF-*x* (*x* = 1−3), where MOROF refers to metal−organic radical open framework) with interesting magnetic properties and additional porosity characteristics.[36−38] However, even though the magnetic behavior of all of these materials has been thoroughly studied, the lack of simple magnetic models has complicated their study and modelization description of the magnetic-exchange interactions between metal ions and carboxylic-based PTM radicals. For this reason, simultaneously, we have also obtained and studied a series of mononuclear complexes as magnetic models. Initially, we reported the preparation of mononuclear Cu(II) complexes with the monocarboxylated PTM radical (PTMMC), for which antiferromagnetic magnetic-exchange interactions (2*J*) in the range of −30 to −50 K between the Cu^{II} ion and the PTMMC radical were determined.[39,40] To expand these studies, herein, we present the synthesis, X-ray analysis, and magnetic properties of the family of first-row transition-metal complexes $[Zn(PTMMC)_2(py)_2(H_2O)_2]\cdot 2EtOH$ (**1**), $[Ni(PTMMC)_2(py)_3(H_2O)]\cdot hexane\cdot 2THF$ (**2**), and $[Co(PTMMC)_2(py)_3(H_2O)]\cdot hexane\cdot 2THF$ (**3**), where the spin moment of the metal varies gradually in the order $S = 0$ [Zn(II)], $S = 1$ [Ni(II)], and $S = 3/2$ [Co(II)]. The results will be also compared to those obtained for a related Cu(II) ($S = 1/2$) complex.

Chart 1

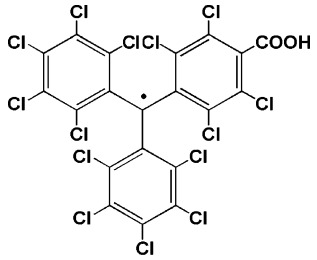

PTMMC

Experimental Section

A. General Considerations. Solvents were distilled before use. In particular, THF was dried over sodium/benzophenone and distilled under argon. All of the reagents were used as received,

(13) Marlin, D. S.; Hill, E.; Weyhermüller, T.; Rentschler, E.; Wieghardt, K. *Angew. Chem., Int. Ed.* **2002**, *41*, 4775.
(14) Zhang, L.; Li, L.-C.; Liao, D.-Z.; Jiang, Z.-H.; Yan, S.-P.; Shen, P.-W. *Inorg. Chim. Acta.* **2001**, *320*, 141.
(15) Vostrikova, K. E.; Luneau, D.; Wernsdorfer, W.; Rey, P.; Verdaguer, M. *J. Am. Chem. Soc*. **2000**, *122*, 718.
(16) Caneschi, A.; Gatteschi, D.; Renard, J. P.; Rey, P.; Sessoli, R. *Inorg. Chem.* **1989**, *28*, 2940.
(17) Inoue, K.; Iwamura, H. *J. Am. Chem. Soc.* **1994**, *116*, 3174.
(18) Aoki, C.; Ishida, T.; Nogami, T. *Inorg. Chem.* **2003**, *42*, 7616.
(19) Yamamoto, Y.; Suzuki, T.; Kaizaki, S. *Dalton Trans.* **2001**, 1566.
(20) Caneschi, A.; Gatteschi, D.; Lalioti, N.; Sangregorio, C.; Sessoli, R.; Venturi, G.; Vindigni, A.; Rettori, A.; Pini, M. G.; Novak, M. A. *Angew. Chem., Int. Ed.* **2001**, *40*, 1760.
(21) Ruiz-Molina, D.; Sporer, C.; Wurst, K.; Jaitner, P.; Veciana, J. *Angew. Chem., Int. Ed.* **2000**, *39*, 3688.
(22) Minguet, M.; Luneau, D.; Lhotel, E.; Villar, V.; Paulsen, C.; Amabilino, D. B.; Veciana, J. *Angew. Chem., Int. Ed.* **2002**, *41*, 586.
(23) Hicks, R. G.; Lemaire, M. T.; Thompson, L. K.; Barclay, T. M. *J. Am. Chem. Soc.* **2000**, *122*, 8077.
(24) Barclay, T. M.; Hicks, R. G.; Lemaire, M. T.; Thompson, L. K. *Chem. Commun.* **2000**, 2141.
(25) Shultz, D. A.; Vostrikova, K. E.; Bodnar, S. H.; Koo, H.-J.; Whangbo, M.-H.; Kirk, M. L.; Depperman, E. C.; Kampf, J. W. *J. Am. Chem. Soc.* **2003**, *125*, 1607.
(26) Ruiz-Molina, D.; Veciana, J.; Wurst, K.; Hendrickson, D. N.; Rovira, C. *Inorg. Chem.* **2000**, *39*, 617.
(27) Ghosh, P.; Begum, A.; Herebian, D.; Bothe, E.; Hildenbrand, K.; Weyhermüller, T.; Wieghardt, K. *Angew. Chem., Int. Ed.* **2003**, *42*, 563.
(28) Pokhodnya, K. I.; Petersen, N.; Miller, J. S. *Inorg. Chem.* **2002**, *41*, 1996.
(29) Gandelman, M.; Rybtchinsky, B.; Ashkenazi, N.; Gauvin, R. M.; Milstein, D. *J. Am. Chem. Soc.* **2001**, *123*, 5372.
(30) Karasawa, S.; Kumada, H.; Koga, N.; Iwamura, H. *J. Am. Chem. Soc.* **2001**, *123*, 9685.
(31) Ballester, M. *Acc. Chem. Res.* **1985**, *12*, 380.
(32) Maspoch, D.; Catala, L.; Gerbier, P.; Ruiz-Molina, D.; Vidal-Gancedo, J.; Wurst, K.; Rovira, C.; Veciana, J. *Chem.—Eur. J.* **2002**, *8*, 3635.
(33) Maspoch, D.; Domingo, N.; Ruiz-Molina, D.; Wurst, K.; Tejada, J.; Rovira, C.; Veciana, J. *J. Am. Chem. Soc.* **2004**, *126*, 730.
(34) Maspoch, D.; Domingo, N.; Ruiz-Molina, D.; Vaughan, G.; Wurst, K.; Tejada, J.; Rovira, C.; Veciana, J. *Angew. Chem., Int. Ed.* **2004**, *43*, 1828.
(35) Roques, N.; Maspoch, D.; Domingo, N.; Ruiz-Molina, D.; Wurst, K.; Tejada, J.; Rovira, C.; Veciana, J. *Chem. Commun.* **2005**, 4801.
(36) Maspoch, D.; Ruiz-Molina, D.; Wurst, K.; Domingo, N.; Cavallini, M.; Biscarini, F.; Tejada, J.; Rovira, C.; Veciana, J. *Nature Mater.* **2003**, *2*, 190.
(37) Maspoch, D.; Ruiz-Molina, D.; Wurst, K.; Rovira, C.; Veciana, J. *Chem. Commun.* **2004**, 1164
(38) Maspoch, D.; Domingo, N.; Ruiz-Molina, D.; Wurst, K.; Vaughan, G.; Lloret, F.; Tejada, J.; Rovira, C.; Veciana, J. *Chem. Commun.* **2005**, 5035.
(39) Maspoch, D.; Ruiz-Molina, D.; Wurst, K.; Rovira, C.; Veciana, J. *Chem. Commun.* **2002**, 2958.
(40) Maspoch, D.; Ruiz-Molina, D.; Vidal-Gancedo, J.; Wurst, K.; Rovira, C.; Veciana, J. *Dalton Trans.* **2004**, 1073.

and they were purchased from Aldrich, Panreac, and Fluka. The PTMMC radical was synthesized according to the procedure previously described.[41] All reactions were carried out in the dark. Microanalyses were performed at the Servei d'Analisi of the Universitat Autònoma de Barcelona. The FT−IR spectra were measured on a Perkin-Elmer Spectrum One spectrometer.

B. Synthesis of $[Zn(PTMMC)_2(py)_2(H_2O)_2]\cdot 2EtOH$ (1). A solution containing 3 mL of pyridine in 15 mL of ethanol was layered onto a solution of PTMMC (0.075 g, 0.095 mmol) and $Zn(NO_3)_2\cdot 6H_2O$ (0.014 g, 0.047 mmol) in 13 mL of ethanol and 2 mL of water. Slow diffusion over 46 days yielded red plate crystals of **1**. Yield: 0.055 g (61%). Anal. Calcd for $C_{54}H_{26}O_8Cl_{28}N_2Zn$: C, 34.34; H, 1.37; N, 1.48. Found: C, 34.99; H, 0.60; N, 1.45. FT−IR (KBr, cm^{-1}): 3426 (w), 2924 (w), 1741 (w), 1643 (m), 1608 (s), 1490 (w), 1449 (m), 1400 (m), 1349 (m), 1334 (s), 1324 (s), 1260 (s), 1221 (m), 1072 (w), 1044 (w), 915 (w), 875 (w), 819 (w), 811 (w), 753 (w), 768 (w), 733 (w), 713 (w), 695 (m), 672 (w), 642 (w), 618 (m), 577(w), 535 (w), 522(w).

C. Synthesis of $[Ni(PTMMC)_2(py)_2(H_2O)_2]\cdot$hexane$\cdot$2THF (2). A solution of $Ni(O_2CMe)_2\cdot 4H_2O$ (0.012 g, 0.049 mmol) in 2 mL of water was dropwise added to a solution of 10 mL of ethanol and 0.5 mL of ether of PTMMC (0.075 g, 0.098 mmol) and stirred for 15 min at room temperature. A red microcrystalline solid was isolated through filtering and dissolved in 8 mL of THF. A solution of 8 mL of hexane containing 3 mL of pyridine was then layered onto the solution of THF. Slow diffusion over 7 days yielded red prism crystals of **2**. Yield: 0.035 g (34%). Anal. Calcd for $C_{69}H_{47}O_7Cl_{28}N_3Ni$: C, 39.82; H, 2.26; N, 2.02. Found: C, 39.46; H, 1.93; N, 1.77. FT−IR (KBr, cm^{-1}): 3434 (w), 2951 (w), 2923 (w), 2856 (w), 1621 (m), 1603 (m), 1582 (w), 1498 (w), 1445 (m), 1402 (w), 1350 (m), 1335 (s), 1323 (s), 1259 (m), 1219 (w), 1142 (w), 1069 (w), 1042 (w), 820 (w), 812 (w), 763 (m), 733 (m), 716 (m), 706 (m), 673 (w), 640 (m), 616 (w), 579 (w), 537 (w), 521 (m).

D. Synthesis of $[Co(PTMMC)_2(py)_2(H_2O)_2]\cdot$hexane$\cdot$2THF (3). A solution of $Co(O_2CMe)_2\cdot 4H_2O$ (0.012 g, 0.049 mmol) in 1 mL of water was dropwise added to a solution of 25 mL of ethanol and 1 mL of ether of PTMMC (0.075 g, 0.098 mmol) and stirred for 15 min at room temperature. The solution was undisturbed for 26 days, and a red microcrystalline solid was isolated through filtering and dissolved in 8 mL of THF. A solution of 8 mL of hexane containing 3 mL of pyridine was then layered onto the solution of THF. Slow diffusion over 26 days yielded red prism crystals of **3**. Yield: 0.043 g (42%). Anal. Calcd for $C_{69}H_{47}O_7Cl_{28}N_3Co$: C, 39.81; H, 2.26; N, 2.02. Found: C, 39.76; H, 2.43; N, 2.32. FT−IR (KBr, cm^{-1}): 3436 (w), 2953 (w), 2924 (w), 2856 (w), 1621 (m), 1602(m), 1489 (w), 1467 (w), 1444 (m), 1403 (m), 1351 (m), 1335 (s), 1323 (s), 1260 (m), 1221 (w), 1069 (w), 1042 (w), 1011(w), 820 (w), 762 (m), 734 (m), 717 (m), 707 (m), 674 (w), 640 (m), 616 (w), 578 (w), 537 (w), 521 (m).

E. X-ray Crystal and Molecular Structural Analyses. Crystal data and details of data collection are summarized in Table 1. X-ray single-crystal diffraction data for complexes **1**, **2**, and **3** were collected on a Nonius KappaCCD diffractometer with an area detector and graphite-monochromated Mo Kα radiation ($\lambda = 0.7106$ Å). Intensities were integrated using DENZO and scaled with SCALEPACK. Several scans in the ϕ and ω directions were made to increase the number of redundant reflections, which were averaged in the refinement cycles. This procedure replaces an empirical absorption correction. The structures were solved and refined using the SHELXTL software.[42] For **1**, the refinement runs in a normal way; all non-hydrogen atoms were refined with anisotropic displacement parameters, and all hydrogen atoms were calculated. The high R value of **1** was caused by a systematic twining and low diffraction of a small crystal. In the refinement of **2** and **3**, the hydrogen atoms were omitted because of poor crystal quality from disordering problems. In the asymmetric unit of **2** and **3**, there is only a half of a molecule, and the $Ni(py)_3(H_2O)$ or $Co(py)_3(H_2O)$ unit lies near a symmetry center, which produces a second $Ni(py)_3(H_2O)$ unit in a 1:1 disorder with a theoretical Ni(1)−NI(1a) distance of 0.97 Å and a Co(1)−Co(1a) distance of 1.34 Å for **3**. As a consequence of this disorder, all atoms were refined with an occupancy of 0.5 and with the two py rings in opposite directions; N(1)C(21)−C(25) and N(1a)C(21a)−C(25a) are in nearly overlying positions by the inversion center with distorted displacement parameters. The carboxylic group is also 1:1 disordered, whereas the residual of the PTMMC radical is well-ordered. Because of this disorder, some atoms must be refined with isotropic displacement parameters. All solvent molecules, which show also disordered positions, were refined isotropically for **2** and **3**.

Table 1. Crystal Data and Structure Refinement for **1**, **2**, and **3**

	1	**2**	**3**
formula	$ZnC_{54}H_{26}Cl_{28}N_2O_8$	$NiC_{69}H_{47}Cl_{28}N_3O_7$	$CoC_{69}H_{47}Cl_{28}N_3O_7$
fw	1888.74	2081.41	2081.63
crystal system	monoclinic	triclinic	triclinic
space group	$P2_1/c$	$P\bar{1}$	$\bar{P}1$
a (Å)	24.760(2)	8.7655(2)	8.7841(5)
b (Å)	8.6933(8)	14.3542(5)	14.3788(9)
c (Å)	17.0695(9)	17.5463(6)	17.3790(9)
α (°)	90	88.461(2)	86.569(3)
β (°)	104.396(5)	80.063(2)	79.914(4)
γ (°)	90	88.448(2)	88.367(4)
V (Å^3)	3558.8(5)	2173.24(12)	2156.9(2)
Z	2	1	1
ρ_{calcd} (g cm^{-3})	1.763	1.590	1.603
λ (Å)	0.71069 (Mo Kα)	0.71069 (Mo Kα)	0.71069 (Mo Kα)
μ (mm^{-1})	1.449	1.135	1.117
T (K)	233(2)	233(2)	233(2)
GOF	1.086	1.180	1.064
R^a, $I > 2\sigma(I)$	11.50	10.27	12.15
$R_w{}^b$, $I > 2\sigma(I)$	32.18	22.80	32.37

$^a R = \sum||F_0| - |F_c||/\sum|F_0|$. $^b R_w = [(\sum w(|F_0| - |F_c|)^2/\sum wF_0{}^2)]^{1/2}$.

F. Magnetic Measurements. Magnetic susceptibility data were obtained for microcrystalline samples of complexes **1**−**3** in the 2−300 K temperature range with a Quantum Design MPMS superconducting SQUID magnetometer operating at a field strength of 0.1−1 T. The data were corrected for diamagnetism of the constituent atoms using Pascal constants.

Results and Discussion

A. Synthesis. The monocarboxylic polychlorotriphenylmethyl radical, PTMMC, was prepared as previously described.[41] Then, a slow diffusion of an excess of pyridine in ethanol in a solution of PTMMC and $Zn(NO_3)_2\cdot 6H_2O$ in

(41) Ballester, M.; Castañer, J.; Riera, J.; Ibañez, A.; Pujadas, J. *J. Org. Chem.* **1982**, *47*, 259.

(42) Sheldrick, G. M. *SHELXL-97, Program for Crystal Structure Refinement*; University of Göttingen: Göttingen, Germany, 1997.

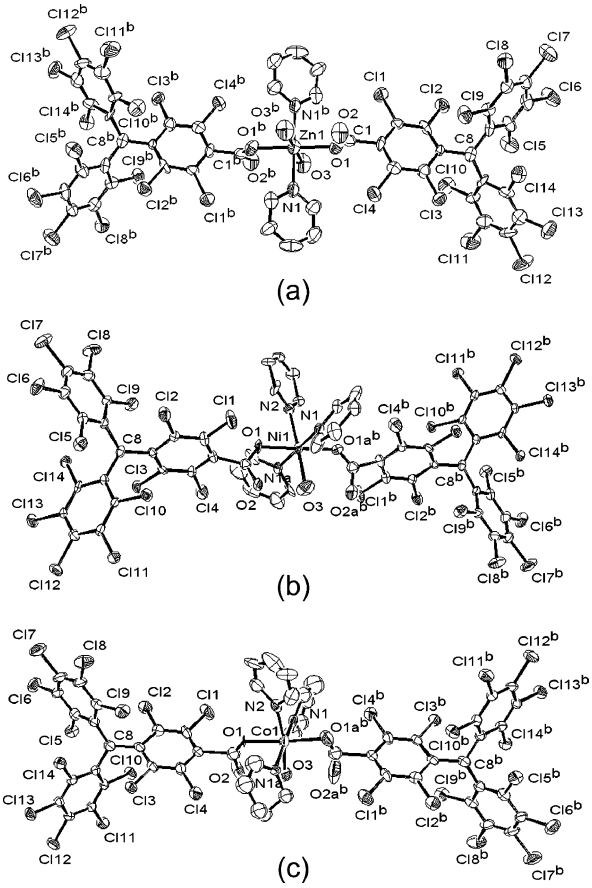

Figure 1. ORTEP plot of PTM-based complexes Zn(II) **1** (a), Ni(II) **2** (b), and Co(II) **3** (c) at the 30% probability level.

ethanol and water yielded high-quality crystals of complex **1** suitable for single-crystal X-ray diffraction analysis. Afterward, slow diffusion of an ethanolic solution of PTMMC in a solution of the Co(II) or Ni(II) metal acetate hydrates yielded, in both cases, a microcrystalline solid, which was isolated by filtration. Then, a solution of pyridine in hexane was diffused into a THF solution of the corresponding microcrystalline solid to yield stable crystals of **2** and **3** suitable for single-crystal X-ray diffraction. All three reactions afforded mononuclear metal complexes, analogous to the already reported mononuclear Cu(II) complex $[Cu(PTMMC)_2(py)_3]\cdot 2.5$hexane **4**, which will be also revised from now on for comparison purposes.[40] The tendency to form mononuclear complexes instead of clusters of higher nuclearity is attributed to the extreme steric demand of the bulky PTMMC ligands with several chlorine atoms, particularly of those located at the ortho positions of the carboxylate group. Similar arguments can be recalled to explain the trans configuration of the two PTMMC ligands in all three complexes.

B. X-ray Crystal Structure. The ORTEP plots of the Zn(II) **1**, Ni(II) **2**, and Co(II) **3** complexes are shown in Figure 1. Selected bond lengths (Å) and angles (°) for **1**−**3** are given in Table 2. As can be seen in Figure 1, complexes **1**, **2**, and **3** are octahedrally coordinated by two monodentated PTMMC radicals, two (or three) pyridine ligands, and two (or one) water molecules.

In complex **1**, the Zn(II) ion lies on a crystallographic inversion center with both PTMMC radicals coordinated in a monodentate mode and with Zn−O(1) bond lengths of 2.088(16) Å and a O(1)−Zn−O(1) angle of 180° (Figure 1a). This leads to a linear PTMMC−Zn(II)−PTMMC (S=1/2···S=0···S=1/2) system, similar to that observed for the Cu(II) complex **4**, with an intramolecular distance between central methyl carbon atoms [C(8)] of both PTMMC ligands, where most of the spin density is localized, of 17.09 Å. The metal ions Ni(II) and Co(II) in complexes **2** and **3**, respectively, also display an octahedral coordination geometry by binding to the oxygen atoms of two distinct PTMMC ligands in a monodentate mode, three nitrogen atoms of the pyridine ligands and one oxygen atom of a water molecule (Figure 1b and c). Therefore, they also exhibit the quasilinear PTMMC−metal−PTMMC motif with three electronic, open-shell units showing metal−O(PTMMC) bond lengths of 2.091(19) and 1.92(2) Å and O(PTMMC)−metal−O(PTMMC) angles ranging from 177 to 167°. In both complexes, the distances between the methyl central carbons [C(8)] of the PTMMC ligands and the metal ions are 8.5−8.7 Å, and the two central carbons are separated by 17.0 and 17.3 Å in **2** and **3**, respectively.

Crystal packing of complex **1** reveals that all of the trimeric PTMMC−metal−PTMMC units are 3-D packed through 26 short chlorine−chlorine contacts, ranging from 3.34 to 3.50 Å, nonclassical C_{py}−H···O hydrogen bonds, and very weak $\pi-\pi$ interactions (see Figure 2). The crystal structure is completed with two ethanol solvent molecules that are strongly hydrogen-bonded with the noncoordinative oxygen atoms of carboxylate groups (O···O 2.88 Å), resulting in the lack of empty voids. On the contrary, the 3-D crystal packing of complexes **2** and **3** leads to the formation of micropores stabilized through 12 Cl···Cl contacts ranging from 3.39 to 3.46 Å. Indeed, as can be seen in Figure 2, this self-assembly generates one-dimensional, rectangular channels along the [100] direction, with dimensions of 7.0 × 3.0 Å when van der Waals's radii are considered. These pores are filled with hexane and THF molecules. The void volumes of the cavities are 632 Å^2, which equals 30% of the unit cell volume.

C. Magnetic Properties. Magnetic data for crystalline samples of complexes **1**−**3** were obtained on a SQUID susceptometer in the temperature range of 2.0−300 K at a constant field of 0.1 and 1 T. The magnetic coupling, 2J, between the magnetic centers was determined by using the Heisenberg Hamiltonian shown in eq 1 on the basis of the quasilinear trimeric magnetic model (radical−metal ion−radical), shown in Scheme 1.[43]

$$H = -2J(S_1\cdot S_2 + S_2\cdot S_3) - 2J_{13}S_1\cdot S_3 \qquad (1)$$

1. [Zn(PTMMC)$_2$(py)$_2$(H$_2$O)$_2$]·2EtOH (1). The $\chi_M T$ versus T plot is shown in Figure 3. As can be seen there, complex **1** follows a typical Curie behavior in the 5−300 K temperature range, with a $\chi_M T$ value that fully agrees with

(43) Ménage, S.; Vitols, S. E.; Bergerat, P.; Codjovi, E.; Kahn, O.; Girerd, J. J.; Guillot, M.; Solans, X.; Calvet, T. *Inorg. Chem.* **2001**, *40*, 2666.

Table 2. Selected Bond Distances (Å) and Bond Angles (°) of **1**, **2**, and **3**

1[a]	**2**	**3**
	Bond Distances	
Zn(1)−O(1) 2.088(16)	Ni(1)−O(1) 2.091(19)	Co(1)−O(1) 1.92(2)
Zn(1)−N(1) 2.16(2)	Ni(1)−O(1a) 2.14(2)	Co(1)−O(1a) 2.14(2)
Zn(1)−O(3) 2.203(17)	Ni(1)−N(1) 2.13(2)	Co(1)−N(1) 2.12(2)
	Ni(1)−N(2) 2.09(2)	Co(1)−N(2) 2.15(3)
	Ni(1)−N(1a) 2.096(19)	Co(1)−N(1a) 2.14(2)
	Ni(1)−O(3) 2.05(3)	Co(1)−O(3) 2.06(2)
	Bond Angles	
O(1)−Zn(1)−O(1) 180	O(1)−Ni(1)−O(1a) 177.1(8)	O(1)−Co(1)−O(1a) 167(2)
O(1)−Zn(1)−N(1) 88.8(7)	O(1)−Ni(1)−N(1) 90.8(10)	O(1)−Co(1)−N(1) 96.4(12)
O(1)−Zn(1)−N(1) 91.2(7)	O(1)−Ni(1)−N(2) 87.7(8)	O(1)−Co(1)−N(2) 83.5(10)
O(1)−Zn(1)−O(3) 88.5(6)	O(1)−Ni(1)−N(1a) 88.0(8)	O(1)−Co(1)−N(1a) 83.5(12)
O(1)−Zn(1)−O(3) 91.5(6)	O(1)−Ni(1)−O(3) 89.3(9)	O(1)−Co(1)−O(3) 87.3(11)
N(1)−Zn(1)−N(1) 180	O(1a)−Ni(1)−N(1) 90.9(9)	O(1a)−Co(1)−N(1) 92.3(14)
N(1)−Zn(1)−O(3) 88.1(7)	O(1a)−Ni(1)−N(2) 90.7(8)	O(1a)−Co(1)−N(2) 85.7(18)
N(1)−Zn(1)−O(3) 91.9(7)	O(1a)−Ni(1)−N(1a) 90.4(8)	O(1a)−Co(1)−N(1a) 90.0(13)
O(3)−Zn(1)−O(3) 180	O(1a)−Ni(1)−O(3) 92.3(9)	O(1a)−Co(1)−O(3) 103.8(19)
	N(1)−Ni(1)−N(2) 92.1(9)	N(1)−Co(1)−N(2) 95.4(11)
	N(1)−Ni(1)−N(1a) 177.0(9)	N(1)−Co(1)−N(1a) 168.5(9)
	N(1)−Ni(1)−O(3) 86.8(11)	N(1)−Co(1)−O(3) 83.4(12)
	N(2)−Ni(1)−N(1a) 90.5(9)	N(2)−Co(1)−N(1a) 96.0(10)
	N(2)−Ni(1)−O(3) 176.9(9)	N(2)−Co(1)−O(3) 170.5(9)
	N(1a)−Ni(1)−O(3) 90.4(11)	N(1a)−Co(1)−O(3) 85.1(11)

[a] Zn(1) lies on a inversion center.

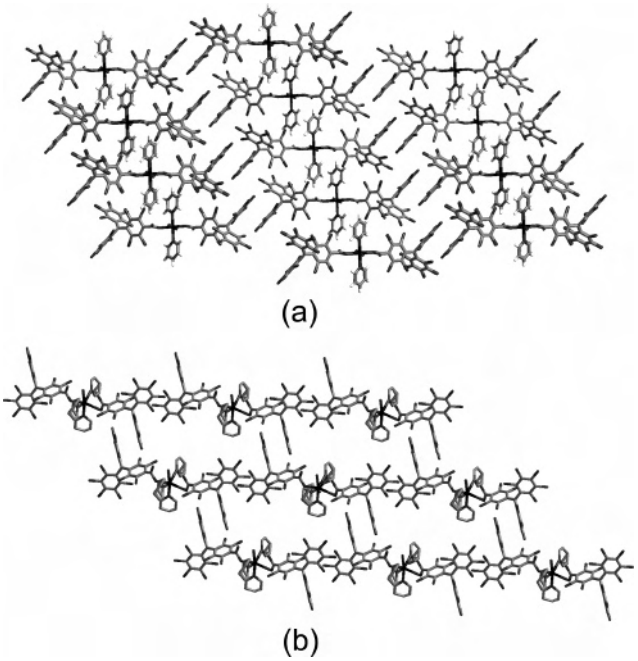

Figure 2. Crystal packing of PTM-based complexes **1** (a) and **2** (b), showing the rectangular, one-dimensional channels exhibited for **2** and **3**. Solvent molecules have been omitted for clarity.

the theoretical value of 0.750 emu·K^{-1}·mol^{-1} expected for two uncorrelated $S = 1/2$ moieties with $g = 2.0$. At low temperatures, the $\chi_M T$ value decreases consistently with the presence of weak inter- and/or intramolecular antiferromagnetic interactions, but no maximum in the susceptibility curve was observed. Fit of the magnetic data was done by using the Hamiltonian described in eq 1, although it was reduced to the expression $H = -2J_{13}S_1 \cdot S_3$ (Bleaney−Bowers expression for the magnetic susceptibility of a dimer of $S = 1/2$)[44] since $S_2 = 0$ for the Zn(II) metal ion. When g_{PTM} was fixed

Scheme 1

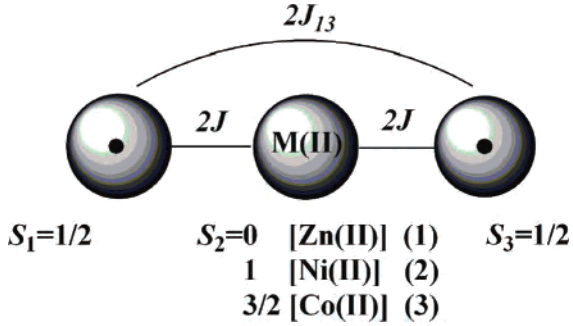

at 2.00 for the PTMMC radical moieties, the least-squares fitting gave the best-fit parameter of $2J_{13} = -1.0$ K. Such small interactions may arise both from intra- and/or intermolecular interactions. Nevertheless, considering the extremely long intramolecular distance (17.09 Å) between both central methyl carbon atoms [C(8)] of the PTMMC units and the agreement of the coupling value with those previously described for intermolecular interactions in purely organic PTM-based crystals due to the Cl···Cl contacts,[41] antiferromagnetic interactions in complex **1** have been

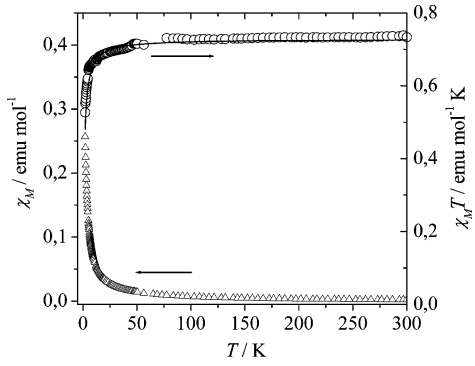

Figure 3. Temperature dependence of the magnetic molar susceptibility of Zn(II) complex **1**, in the forms of χ_M versus T (triangles) and $\chi_M T$ versus T (circles). Black, solid line represents the best-fit calculated data.

(44) Bleaney, B.; Bowers, K. D. *Proc. R. Soc. London, Ser. A* **1952**, *214*, 451.

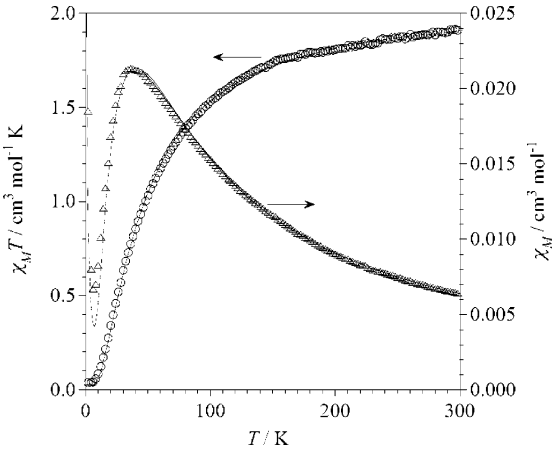

Figure 4. Temperature dependence of the magnetic molar susceptibility of Ni(II) complex **2**, in the forms of χ_M versus T (triangles) and $\chi_M T$ versus T (circles). Black, solid line represents the best-fit calculated data.

assigned to the presence of intermolecular antiferromagnetic interactions through the large number of Cl···Cl contacts found in its crystal packing. In fact, it is possible to reproduce the magnetic susceptibility data very well using the Curie−Weis law

$$\chi_M = \frac{N\beta^2 g^2}{2K(T-\theta)} \text{ with } g_{PTM} = 2.00 \text{ and } \theta = -1.0 \text{ K}$$

2. [Ni(PTMMC)$_2$(py)$_3$(H$_2$O)]·hexane·2THF (2). The temperature dependence of the molar magnetic susceptibility, χ_M, together with its corresponding $\chi_M T$ product for complex **2** is shown in Figure 4. The observed χ_MT value of 1.93 cm^3·K·mol^{-1} at 300 K is close to that expected for a noninteracting Ni(II) ion ($S = 1$ and $g_{Ni} = 2.3$; vide infra) and two independent PTMMC radical units ($S = 1/2$ and $g_{PTM} = 2.00$). Upon lowering the temperature, $\chi_M T$ decreases smoothly until 100 K, from where there is a more pronounced decrease down to a constant value of 0.03 cm^3·K·mol^{-1} below 5.0 K. Although, in a usual scheme of spin coupling, the ground spin state would correspond to a singlet, $S = 0$; in the present case, this ground state is magnetic ($\chi_M T$ ca. 0.03 cm^3·K·mol^{-1}) because of the different values of the local g factors ($g_{Ni} > g_{PTM}$) that yield uncompensated magnetic moments. The increase of the magnetic susceptibility below the temperature of its maximum is also due to these uncompensated magnetic moments and not necessarily to the usual claimed presence of magnetic impurities. The presence of small amounts of paramagnetic impurities would produce a similar behavior. The strong correlation of both factors precludes an accurate analysis of their influence.

Fit of the magnetic data was done by diagonalization of the Hamiltonian of eq 2, in which exchange interactions between PTMMC radicals are neglected according to the previously described results. In order to take into account the uncompensated magnetic moments due to the different values of the local g factors, it is necessary to diagonalize the Zeeman matrix, and this avoids getting an analytical expression for the magnetic susceptibility.

$$\hat{H} = -2J[\hat{S}_1\hat{S}_2 + \hat{S}_2\hat{S}_3] + g_{PTM}\beta H[\hat{S}_1 + \hat{S}_3] + g_{Ni}\beta H\hat{S}_2 \quad (2)$$

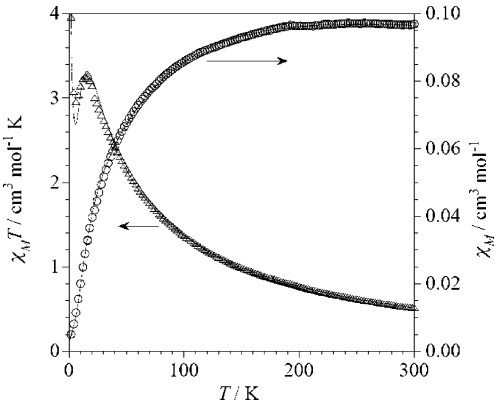

Figure 5. Temperature dependence of the magnetic molar susceptibility of Co(II) complex **3**, in the forms of χ_M versus T (triangles) and $\chi_M T$ versus T (circles). Black, solid line represents the best-fit calculated data.

When $g = 2.00$ for the PTMMC radical moieties, the resulting parameters for the best fit ($R = 2.7 \times 10^{-5}$) were $2J/k_B = -47.1$ K and $g_{Ni} = 2.32$. Thus, this value is very similar to that observed for the related Cu(II) complex, in which a Cu(II)−PTMMC magnetic-exchange interaction of $2J/k_B = -42$ K was determined.[40] This confirms the ability of such carboxylic-based PTM radicals to transmit moderate antiferromagnetic interactions when they participate as ligands with transition-metal ions with such a linear configurations.

3. [Co(PTMMC)$_2$(py)$_3$(H$_2$O)]·hexane·2THF (3). The temperature dependence of the $\chi_M T$ product for complex **3** is shown in Figure 5. The observed $\chi_M T$ value of 3.88 emu·K·mol^{-1} at 300 K is much higher than the expected spin-only value for a Co(II) ion ($S = 3/2$) and two PTMMC radical units ($S = 1/2$), implying the presence of a significant orbital contribution. Upon lowering the temperature, the $\chi_M T$ value decreases continuously down to 0.22 emu·K·mol^{-1} at 2.0 K. The decrease at high temperature is due to the presence of an antiferromagnetic interaction between the PTMMC and Co(II) ion as well as to the depopulation of the higher energy Kramer's doublets of the Co(II) center with a $^4T_1$ term for the ground state. At low temperature ($T < 20$ K), only the ground Kramer's doublet is populated, and it can be regarded as an effective spin doublet, $S_{eff} = 1/2$, with a g value which is in the range of $g_{eff}^{Co} = 3.8-4.3$.[45,46] Therefore, the value of the $\chi_M T$ product of the ground spin state for **3** can be estimated from

$$(\chi_M T)_{LT} = \frac{N\beta^2 g^2}{3k}[(2S_{PTM} - S_{eff}^{Co})^2 + |2S_{PTM} - S_{eff}^{Co}|] \text{ with } g = \frac{4g_{PTM} - g_{eff}^{Co}}{3}$$

A value of $\chi_M T = 0.2-0.14$ emu·K·mol^{-1} at low temperature is expected for $g_{PTM} = 2.0$, $g_{eff}^{Co} = 3.8-4.3$, and $S_{PTM} = S_{eff}$

(45) Herrera, J. M.; Bleuzen, A.; Dromzée, Y.; Julve, M.; Lloret, F.; Verdaguer, M. *Inorg. Chem.* **2003**, *42*, 7052.
(46) Rodriguez, A.; Sakiyama, H.: Masciocchi, N.; Galli, S.; Galez, N.; Lloret, F.; Colacio, E. *Inorg. Chem.* **2005**, *44*, 8399.
(47) Mishra, V.; Lloret, F.; Mukherjee, R. *Inorg. Chim. Acta* **2006**, *359*, 4053.

$= 1/2$,[48] in agreement with that observed for **3** (0.22 emu·K·mol^{-1}) and showing the existence of a moderately strong antiferromagnetic interaction between the PTMMC and Co(II).

Due to the presence of a first-order orbital momentum in six-coordinated Co(II) ions, the isotropic exchange interaction, Heisenberg−Dirac−van Vleck model (eq 1), is insufficient to discuss Co(II) complexes and must be supplemented by consideration of orbitally dependent exchange interactions as well as spin−orbit coupling effects.[47]

The Hamiltonian describing the spin−orbit coupling is given by eq 3

$$\hat{H}_{SO} = -\alpha\lambda\hat{L}\hat{S} \tag{3}$$

where λ is the spin−orbit coupling and where α is an orbital reduction factor defined as $\alpha = A{\cdot}\kappa$. The κ parameter considers the reduction of the orbital momentum caused by the delocalization of the unpaired electrons, and A contains the admixture of the upper $^4T_{1g}(^4P)$ state into the $^4T_{1g}(^4F)$ ground state ($A = 1.5$ and 1 for the weak and strong crystal field limits, respectively).[45] In the frame of the T_{1g} and P terms' isomorphism, $L(T_{1g}) = -AL(P)$, we can use $L = 1$ and treat eq 3 as an isotropic Hamiltonian describing the interaction between two angular moments, $L = 1$ and $S = 3/2$, being the $-\alpha\lambda$ coupling parameter.

Moreover, in **3**, the Co(II) ion presents a distorted octahedral surrounding. Under an axial distortion, the triplet orbital $^4T_{1g}$ ground state splits into a singlet $^4A_2$ and a doublet ^4E level with an energy gap of Δ, this gap being positive when the orbital singlet is the lowest. The one-center operator responsible for such an axial distortion can be expressed by the Hamiltonian (eq 4), which represents the zero-field splitting of the triplet $L = 1$.[45]

$$\hat{H}_{ax} = \Delta\left[\hat{L}_Z{}^2 - \frac{1}{3}L(L+1)\right] \tag{4}$$

Therefore, the full Hamiltonian describing the magnetic properties of **3** is given in eq 5, where the two last terms are the Zeeman interaction and where the first one is the magnetic exchange between the spin quartet ($S = 3/2$) from the Co(II) ion and the spin doublets ($S = 1/2$) from each PTMMC radical.

$$\hat{H} = -J(\hat{S}_1^{PTM}\hat{S}_{Co} + \hat{S}_{Co}\hat{S}_2^{PTM}) - \alpha\lambda\hat{L}_{Co}\hat{S}_{Co} + \Delta[\hat{L}_{zCo}^2 - 2/3] + \beta H(-\alpha\hat{L}_{Co} + g_e\hat{S}_{Co}) + \beta H g_{PTM}(\hat{S}_1^{PTM} + \hat{S}_2^{PTM}) \tag{5}$$

No analytical expression for the magnetic susceptibility (which would depend on J, α, λ, and Δ) can be derived. Numerical matrix diagonalization techniques using a Fortran program,[49] conducting extensive mappings with the aim of locating the global minimum of each system among a large number of local minima, allowed us to determine the values of these parameters. The best-fit parameters are $2J/k_B = -15.2$ K, $\alpha = 1.46$ (i.e., $A = 1.5$ and $\kappa = 0.93$), $\lambda/k_B = -187$ K, and $\Delta/k_B = 290$ K ($R = 7.8 \times 10^{-5}$). The calculated curve matches the experimental data very well in all of the temperature ranges and clearly shows the existence of an intramolecular antiferromagnetic interaction between the Co(II) ion and the PTMMC radicals. The values of the parameters obtained by the previous fit are within the range of those reported for high-spin octahedral Co(II) complexes.[45−47]

Conclusions

The reaction of para-substituted monocarboxylic polychlorotriphenylmethyl radical (PTMMC) with different first-row transition-metal ions has generated a series of complexes with Zn(II), Ni(II), Co(II), and Cu(II),[38,39] from which it is demonstrated that metal−radical exchange interactions are moderately antiferromagnetic in nature. In such a context, carboxylic-based PTM radicals turn out to be excellent coordinating paramagnetic ligands to design new metal−organic systems with different magnetic properties. For this reason, actually, further studies to build polynuclear complexes using the PTMMC radical with transition and lanthanide ions or to expand the range of structural motifs, the structural dimensionality and magnetic behaviors of metal−radical complexes based on polychlorinated triphenylmethyl radicals, either mono-, di-, tri-, or hexafunctionalized with carboxylic groups, are currently underway.

Acknowledgment. This work has been supported by the European Community under the Network of Excellence MAGMANet (Contract 515767-2) and the QUEMOLNA Marie Curie Research Training Network (Contract MRTN−CT-2003-504880) and by the Ministerio de Educación y Ciencia (Spain), under Projects MAT2003-04699 and CONSOLIDER-C EMOCIONa (CTQ2006-06333/BQU) and Generalitat de Catalunya (2005SGR00362). D.M. acknowledges the Ministerio de Ciencia y Tecnologia for a Ramón y Cajal contract. N.D. is also grateful to the Ministerio de Educación Cultura y Deportes (Spain) for the predoctoral Grant No. AP2000-1842 of the FPU program.

Supporting Information Available: ESR spectra for complexes **1**, **2**, and **3**. This material is available free of charge via the Internet at http://pubs.acs.org.

IC061815X

(48) Kahn, O. *Molecular Magnetism*; VCH: Weinheim, Germany, 1993.

(49) Cano, J.; *VPMAG Package*; University of Valencia: Valencia, Spain, 2003.